JOINT EUROPEAN TORUS JET

JET–P(87)04

P.E. Stott

Review of JET Diagnostics and Results

Review of JET Diagnostics and Results

P.E. Stott

JET-Joint Undertaking, Culham Science Centre, OX14 3DB, Abingdon, UK

Preprint of Paper to be presented ath the Course on Basic and Advanced Fusion Plasmas Diagnostic Techniques, Varenna, Italy 1986

into a single discharge is ~ 18MW.

With ohmic heating, peak ion and electron temperatures of 3keV and 4keV respectively are achieved with a plasma density ~ 4.2 $10^{19}m^{-3}$ and energy confinement time τ_E up to 0.8s. With ICRH the peak electron and ion temperatures are increased to about 5.5keV but the energy confinement time drops to about 0.3s. With neutral beam heating there is also a reduction in the energy confinement time but at low central densities $n_e(0) \lesssim 1.5 \times 10^{19}m^{-3}$ central ion temperatures $T_i(0) > 12.5$ keV are obtained. Improved confinement has been recently observed with neutral beam heating in discharges with a divertor-like configuration when the plasma boundary is defined by a magnetic separatrix so that the discharge is no longer in contact with the limiter.

JET started operating in 1983 with a minimum number of basic diagnostic systems. Further systems have been added progressively and the full set of JET diagnostics is now near completion. The present status is summarized in Table 1 which shows that out of a total of 39 systems, 24 are in routine operation, 10 are being installed or commissioned and a further 5 are still to be constructed. A schematic showing the location of diagnostics on the JET machine is shown in figure 1.

In this lecture I will review the present status of the JET diagnostics and give a brief review of recent experimental results.

2. Overview of JET Diagnostic Systems

The design of diagnostic systems for JET started in 1979 and was reviewed at the last Varenna diagnostics meeting in 1982 [5]. Since then there have been a few changes; some new systems have been added and a few systems cancelled, but the majority of the systems now installed and working on JET are those which were described at the meeting four years ago. The time scale to design, construct, install and bring into full reliable operation the diagnostics for a large fusion experiment like JET is substantial. It takes a minimum of two to three years and in some cases as long as six or seven years. Many of these diagnostic systems have been built by the other fusion laboratories who are partners in the JET project. These systems were specified and paid for by the JET project via a series of contracts and this formal relationship was needed

so that the work in the many different laboratories could be effectively co-ordinated and the complex systems could be built to uniform standards. This has been a particularly successful collaboration with the result that the diaghostic expertise of the European Fusion Programme has been concentrated at JET. Many skilled scientists, engineers and technicians have been involved and many people have worked at JET for varying periods to install and operate these systems.

A deliberate policy has been to use diagnostic methods whenever possible whose principals have already been demonstrated on other experiments. However, there are some exceptions where novel diagnostic techniques have been developed and applied on JET. What is new is the sophistication of the application of the established methods to JET and the complexity of the engineering. This has been necessitated by several factors including the large physical size of JET, the need to maintain compatibility with the very high standards of engineering of the other systems of the JET device and by the hostile radiation environment which will occur in discharges with deuterium and tritium. Considerable emphasis has been placed on achieving much higher standards of reliability and accuracy for these diagnostic systems than has previously been the norm in fusion research. All of the JET diagnostic systems are remotely controlled through a computer system and many can be operated automatically with a minimum of skilled operators.

In order to make the most efficient use of experimental time and to improve the self consistancy of the measurements, a complete set of data is measured simultaneously during every discharge. In general we find that the measurements are reproducible from shot to shot for discharges with the same conditions. A large number of spatial channels is needed to measure profiles of plasma parameters with adequate spatial resolution (generally 5-10cm) in these discharges with large poloidal cross-section (2.5 x 4.2m). As the poloidal cross-section of JET discharges is non-circular, those measurements which integrate along a chordal line of sight have to be unfolded by tomographic inversion methods and thus the plasma must be viewed simultaneously in orthogonal directions. In most cases the number and location of the lines of sight are severely constrained by the access to the plasma through the available ports in the vacuum vessel. There are similar considerations in determining the time scales on which data should be recorded. The plasma parameters related to quasi-equilibrium processes (eg.

the energy balance) need to be recorded on time scales which are up to an order of magnitude shorter than the characteristic equilibrium times, eg. recording on time scales of about 10ms is required for equilibrium time scales $\gtrsim$ 100ms. Data is usually recorded at this rate throughout the 20 second period of the JET discharge, ie. typically 2 x 10^3 data points per spatial channel. There are however many transient plasma phenomena which take place on much shorter time scales (eg. instabilities and disruptions) and these data must be recorded on time scales of a few microseconds. Clearly it would not be feasible in terms of data storage to record data on all the measurement channels at a MHz rate for 20s and so the fastest data taking rates are usually switched on for a limited number of time windows centered around periods of interest. These windows may be pre- or post- triggered, in some cases by signals from other diagnostics.

Fairly stringent constraints have had to be applied to the data requirements of each diagnostic to keep the total data recorded per JET discharge within reasonable limits. Presently we record about 7 x10^6 data points per discharge and this is planned to increase to about 1.5 x10^7 when all of the diagnostics are operating. The data is recorded in local CAMAC memories during the discharge and then read into the memories of a network of NORD computers (NORD 500 series) which are used for diagnostic control and for immediate data analysis. Initial analysis and display of results is carried out by these computers in the interval between successive discharges and is used to guide the progress of the experiment. At the same time the complete raw data file is copied into the memory of a large main frame computer system (IBM 3084Q + CRAY XMP) where it can be used for higher level analysis and it is via these computers that the retrospective analysis of JET data is carried out. An important feature is that data for all JET discharges and from all the diagnostics are available to all members of the JET project via this main frame computer.

Magnetic Diagnostics

Measurements of the poloidal magnetic field outside the plasma are used to determine the discharge current, loop volts, ohmic power input, position and shape of the plasma boundary. More detailed analysis of these data yields information on the total plasma energy and pressure, plasma inductance and

the shape of the magnetic surfaces inside the plasma [6]. The magnetic measurement coils (KC1) are shown schematically in Figure 2. The components of the poloidal magnetic field perpendicular to the surface of the vacuum vessel are measured with a set of flux loops on the surface of the vessel [7]. There are two types of loops; full flux loops which make a single turn in the toroidal direction are used in locations where there are no obstructions from ports etc, whilst saddle loops are used in places where there are obstructions. The component of the poloidal field parallel to the vacuum vessel surface is measured with small pick-up coils which are located inside inconel protection tubes on the inside of the vacuum vessel. There are 18 of these pick-up coils distributed around the poloidal circumference and there are identical sets of coils on each of the octants. The signals from these coils are processed electronically and combined in various ways using both analog and digital techniques to yield the various plasma quantities. For example the plasma current is obtained by adding the signals from all the internal pick-up coils to simulate a continuous Rogowski coil. The plasma position and the shape of the outermost magnetic flux surface are determined to a typical accuracy of ±10mm by a numerical solution of the Laplace equation for the poloidal field outside the plasma with the boundary conditions fitted to the field components measured by the magnetic diagnostics. For plasmas with elongated cross-section the internal flux surfaces can be estimated by solving the Grad-Shafranov equation with the outer flux surface as a boundary condition. The integral plasma quantities such as the total kinetic energy, pressure and inductance are obtained from the Shafranov integrals. The coils and flux loops on two of the octants are dedicated for active feedback control of the plasma position, current, shape etc., whilst those on the other six octants are used for diagnostics purposes. The diamagnetic effect is used to determine the perpendicular plasma pressure using a set of coils which is supported on one of the toroidal field coils.

Electron Density

The electron density profiles are measured by interferometry and by reflectometry. The main interferometer is a Far Infra-Red instrument (KG1) with seven vertical and three lateral lines of sight [8,9]. This systems works at a wavelength of 195μm using DCN laser sources. The frequency shift for the reference arm is produced by means of a rotating grating. The optical components of the vertical channels are supported on a massive frame which is

mechanically independent of the rest of the JET machine in order to reduce the effect of vibrations. However, the lateral channels have mirrors which are mounted on the inside of the vacuum vessel and are thus sensitive to vibrations. These channels were designed to operate simultaneously with a second interferometer (wavelength = 3.39μm) in order to compensate for the effect of the mechanical vibrations but unfortunately this system has not worked satisfactorily due to difficulties with the alignment and reflectivity of the internal mirrors at the shorter wavelength. Modifications are in hand to change the second wavelength to 119μm. JET also has a 2mm Microwave Interferometer (KG2) with a single vertical line of sight which is used mainly as a back-up to the Far-Infra-Red Interferometer.

We are also developing Microwave Reflectometry (KG3) [10] as a diagnostic to improve the accuracy of the density profile measurements near to the edge of the discharge where the data from the Far-Infra-Red interferometer is rather sparse and where future changes to the JET machine configuration will cause us to loose one of the vertical channels. Results with a prototype reflectometer have been very encouraging [11] and a multichannel instrument [12] is now being constructed and will be installed on JET during 1987. This instrument will also be used to observe localised density fluctuations.

Electron Temperature

The main methods used for electron temperature measurements are electron Cyclotron Emission (KK1 and KK2) and Thomson Scattering (KE1 and KE3). In addition the X-ray Pulse Height Analysis System (KH2) [13] is used to measure fast electron distributions in runaway or slideaway discharges.

We have invested considerable effort into developing ECE [14] as the main electron temperature diagnostic in JET. A poloidal section of the plasma is viewed along ten different chords by an array of rectangular horn antennae. The ECE radiation (for typical JET parameters in the range 70 - 350GHz) is transmitted from these antennae by oversize rectangular microwave waveguides to the detectors which are located outside the Torus Hall. The distance along the route followed by the waveguides is of the order of 100m and the oversized waveguide is needed for low attenuation of the transmitted signals. Great care is required in the design of bends etc. to avoid serious problems with conversion between different waveguides modes.

Four types of detectors are used.

i) The complete spectrum of the ECE radiation over several harmonics is measured with scanning Michelson Interferometers (scan time ~15ms), and the relative amplitudes of the different harmonics are used to check that the emission is thermal.

ii) The spatial profile of temperature along different chords is measured with Fabry-Perot Interferometers which are scanned over the second harmonic emission in a time of ~3ms. Each scan gives a temperature profile along the chordal line of sight with a spatial resolution ~10cm. By combining the data from different chords a two dimensional distribution can be constructed. The Fabry-Perot instruments can also be operated at fixed frequencies so that the temperatures at selected positions in the plasma can be recorded as a function of time with a sensitivity about 5eV and time resolution about 10μs.

iii) A twelve channel Grating Polychromator (KK2) is used to record the time variation of temperatures at 12 selected positions along a single chord. This is particularly useful for measurements of the propagation of heat perturbations through the plasma following the collapse of an internal sawtooth instability and permits a measurement of the thermal conductivity.

iv) A superheterodyne receiver (KK3) [15] is being developed for measurements of the temperature profile near the plasma edge.

The ECE diagnostics are absolutely calibrated by means of specially developed thermal sources of known temperature and emissivity. These calibration techniques have now been developed to the point where the absolute accuracy of the ECE measurements on JET is estimated to be within ±10% and the relative accuracy between different spatial points on the same profile is within ±5%. These values are confirmed by comparison with the Thomson scattering measurements (Figure 3).

JET will have two Thomson scattering systems, one is already operating and the second is under construction. The first system, which we call the Single Point Thomson Scattering System (KE1), is of conventional geometry (Figure 4), ie. the scattered light is collected in a cone at 90° to the incident light.

The source is a ruby laser which can be operated in a variety of combinations of energy per pulse and repetition rate ranging from a single pulse of 25J to a series of ~25 pulses of 2.5J at 1Hz. The system is limited to a single spatial point measurement per discharge but can be moved to different major radii in between successive discharges. This system has been in operation for two years and has worked very reliably [16,17].

A new type of Thomson Scattering diagnostic (KE3) is being developed for JET and will be installed at the end of 1986. The system will use a laser with a much shorter pulse length (~250ps) than a conventional Thomson scattering laser (~20ns). The scattered light will be recorded continuously as the laser light pulse travels across the plasma. The spatial profile will be determined from the time of flight of the laser pulse whilst temperature and density will be determined respectively from the spectral width and intensity of the scattered light as in a conventional system. This system has been described in detail in another paper at this meeting [18]. The new system will use much of the existing optics of the Single Point system and both systems will be able to operate together.

Ion Temperatures

Ion temperatures are generally more difficult to measure than electron temperatures and all of the available methods encounter some problems and limitations. We have an array of five Neutral Particle Analysers (KR1) which view the poloidal section along different chords [19]. Each instrument has magnetic and electrostatic analysers which disperse the ions in both mass and energy onto on an array of channel multipliers thus measuring simultaneously the hydrogen and deuterium fluxes. These instruments can measure the temperature of the hydrogenic ions, the ratio D^+/H^+, and the fast ion distribution functions during additional heating. However, measurements at high densities are limited by the opacity of the plasma to neutrals escaping from the central plasma. Under these conditions the instruments usually do not measure the central ion temperature directly, and to extrapolate the data to the central region, it is therefore necessary to use a neutral atom transport code.

Two Neutron Spectrometers (KM1 and KM3) are used to measure ion temperatures in deuterium plasmas [20] with ohmic heating or hydrogen neutral beam

injection (they cannot measure temperatures during deuterium beam injection because the neutron production is then dominated by the beam-plasma interactions). At low yields in deuterium plasmas a ^{3}He ionization chamber has been used above the roof of the Torus Hall using a penetration hole through the roof as a collimator. This is a temporary installation and the ionization chamber will be moved later to a large concrete shield and collimator in the torus hall. In the Time-of-Flight Neutron Spectrometer (KM3) neutrons are scattered by protons in the first of a pair of scintillators which are separated by ~1m. The neutron energy is determined by the time-of-flight between the two scintillators. This instrument has higher resolution than the ionization chamber but lower sensitivity and therefore requires a higher neutron flux to be effective.

The velocity distribution of impurity ions is measured spectroscopically with several instruments. The High Resolution Crystal Spectrometer (KX1) is used to observe highly ionized nickel ions in the central core of plasma, typically out to a radius of ~0.5m [21]. It views tangentially and thus also measures the toroidal rotation velocity. The crystal and detector are located outside the Torus Hall on a Rowland circle whose diameter is 24m. Information on the temperature and rotation at the edge of the plasma can also be obtained from the Grazing Incidence Survey Spectrometer (KT4). The temperatures of light impurity ions are measured by Charge Exchange Recombination Spectrometry (KS4) [22] but this instrument can be used only during neutral beam injection heating. (JET does not have a dedicated diagnostic neutral beam). It is planned that the heating neutral beam sources will be modulated in order to improve the ratio of signal to background noise. The present instrument views perpendicularly in the plasma mid-plane and will be later extended to a tangential view over the whole cross-section.

For some discharge conditions there is good agreement between values of ion temperature measured with the different diagnostics (Figure 5), but there are also many discharges where the agreement is less satisfactory for reasons which are still not completely understood.

Impurities

As in most tokamaks, spectroscopic diagnostics are the main methods for identifying the impurities in the plasma and for measuring their

concentrations. The wavelengths of the emitted impurity line radiation cover a very wide spectral range from the visible (~6000A) through the ultraviolet to the soft x-ray region (~1A). Several different instruments are needed to cover this very wide spectral range and some overlap is desirable for cross calibration. The spectral survey is covered by three instruments: a VUV Broad Band Spectrometer (KT2), a Grazing Incidence Survey Spectrometer (KT4) and a Soft X-ray Pulse Height Analysis System (KH2). A Broad Band Crystal Spectrometer (KS1) with two crystals in a periscope-like arrangement with the detector outside the Torus Hall will be installed for the tritium phase of JET operation.

There are also three spectrometer systems which are designed to measure spatial profiles of impurities [23]. The VUV Spatial Scan Spectrometer (KT1) will cover the wavelength range from 2000 to 100A and is based on three identical duochromators. This instrument will view the plasma through rotating grazing-incidence mirrors, with two horizontally viewing instruments and one viewing vertically. Unfortunately the full implementation of this diagnostic has been delayed by a series of vacuum problems in the mechanisms of the rotating mirrors. A Spatial Scan Crystal Spectrometer (KS2) is being constructed and will cover the wavelength range 15 - 25A. This instrument uses two crystals which can be translated and rotated synchronously to scan in wavelength whilst the crystal nearer to the plasma can also be rotated about an orthogonal axis to scan the plasma spatially. This instrument will be installed during 1987. Information on spatial profiles of impurities is also obtained by Charge-Exchange Recombination Spectrometry (KS4).

The fluxes of impurities and hydrogenic atoms entering the plasma from the walls and limiters are measured with Visible Spectrometers (KT3) and H_α Monitors (KS3). The effective ionic change, Z_{eff}, is measured spectroscopically by visible bremstraahlung with a system (KS3) which includes a number of discrete channels and a poloidal array, and also from the intensity of the Soft X-ray Pulse Height Spectrum (KH2).

The power radiated by impurities is measured by two arrays of Bolometers (KB1) which view the plasma in orthogonal directions through small apertures (Figure 6). The horizontal camera has 20 channels and the vertical camera has 14

channels. Each detector consist of a pair of thin film, gold resistors evaporated on to a mylar foil. One resistor receives plasma radiation and the other is shielded from the plasma. The pair are connected in a bridge arrangement to cancel drifts in the substrate temperatures and this arrangement also cancels to first order the effects of neutron and hard x-ray radiation. The radiated power density is obtained by Abel inversion using the shape of flux surfaces derived from the magnetic diagnostics. The radiated power is also measured with an array of Soft X-Ray Diodes (KJ1) which are primarily intended for fluctuation and instability studies. The bolometer and diode arrays are in fact complementary since the X-Ray Diodes are more sensitive the hot central plasma core whilst the bolometers are more sensitive the cooler plasma edge regions.

Plasma Boundary

Direct measurements of the plasma interactions with material surfaces have been made by post-mortem surface analyses of samples removed from the limiter and walls whenever the JET vacuum vessel has been opened for maintenance [24]. These measurements necessarily give an integrated picture over many months of operation but have nevertheless allowed us considerable insight into the processes responsible in JET for impurity production and migration. Probe drive systems are used to expose surface collector probes in the plasma boundary region for single discharges or for a sequence of discharges. These probes have both time and spatial resolution. Two probe drives (KY3) are located on the top of the vacuum vessel and one of these contains a magazine of five interchangeable collector probes which may be removed via a vacuum cassette. There is also a more sophisticated transfer system (KY2) which can be used to expose probes in the horizontal mid-plane of the torus (close to the limiters) and then to transport the samples to a Surface Analysis Station (KY1) where they can be analysed immediately by a variety of techniques. These systems have given preliminary data during 1986 and will come into full operation in 1987.

The same probe drive systems are also used to introduce electrical probes into the boundary regions of the discharge to measure the local plasma densities, temperatures and heat fluxes [25]. These measurements are supplemented by fixed probes which are located in the protective carbon shield surrounding one of the RF antennas. The measurements of plasma densities and temperatures in the edge regions will be extended into the plasma by the new Microwave

Reflectometer (KG3) and Super Heterodyne ECE (KK3) diagnostic systems which have already been discussed.

The surface temperatures of the limiter antenna, inner wall tiles and separatrix plates are measured by infra-red cameras (KL1). Two camera systems are used. The first system is based on CCD cameras which have good spatial resolution [26,27]. This is used to monitor high surface temperatures which could result in thermal damage. However this system has a limited dynamic range and cannot be used to follow the full temperature excursion of the limiter surface during a high powered discharge. A new system is being developed based on an infra-red detector array (sensitive in the wavelength range 3 - 5μm) which will cover a wider temperature range but will have lower spatial resolution.

Neutron and Fusion Products

Considerable effort is being invested in neutron and fusion product diagnostics in view of JET's experimental programme in D-D and D-T plasmas. A particular requirement for the neutron diagnostics is to cover a very wide range of yields from ~10^{10} neutrons s^{-1} in hydrogen discharges (ie. from runaways) to ~10^{19} neutrons s^{-1} (in hot D-T plasmas). The total neutron yield is monitored routinely using ^{235}U and ^{238}U Fission Chambers (KN1) which are mounted in pairs on the JET machine structure. Two new neutron yield diagnostics are just being installed and commissioned. These are two arrays of Collimated Neutron Detectors (KN3) which will measure the spatial profile of the neutron yield and an Activation Transfer System (KN2) which will expose neutron foils close the plasma edge and transfer them pneumatically to a counting station [28].

The neutron spectrometers (KM1 and KM3) for ion temperature measurements in deuterium plasmas have already been described. When these measurements are made simultaneously with the total neutron yield it is possible to determine the deuterion density n_d. Typically we find $0.5 \leq n_d/n_e \leq 0.7$. Construction is now starting on two 14MeV spectrometers (KM2 and KM5) which will be required during the tritium phase of the JET experimental programme. A prototype fusion product diagnostic (KP1) has been tested and has given some very interesting data on the production of energetic protons during ICRH [29]. This development and related work on α particle diagnostics is continuing.

Fluctuations and Instabilities

Many of the diagnostics already discussed are also used with fast time resolution windows to study fluctuations and instabilities. In particular sawteeth are being studied with the ECE diagnostics (KK1 and KK2) and with the Soft X-ray Diode Arrays (KJ1). The diode arrays [30] are mounted inside the JET vacuum vessel in two cameras which view the plasma cross-section in orthogonal directions. The wavelength range of these detectors can be changed by means of thin foil filters which can be introduced in front of the detectors and this has the effect of changing the sensistivity of the system to respond to changes in the plasma temperature and density. Each detector integrates the emission along its line of sight but with such a large number of sight lines (62 horizontal and 38 vertical) it is possible to unfold the integral signals remotely using tomographic methods to produce contour maps of the local soft x-ray emission density. This diagnostic has proved particularly powerful in observing the mechanism of the sawtooth collapse [31].

3. Summary of Experimental Results

JET has now been operating for three years and there has been steady progress in improving plasma operating conditions [32]. Discharges are now run routinely at the full design value of the toroidal magnetic field B_T = 3.4T and with currents up to 5.1MA (Figure 8). The plasma current, position, elongation and shape are all controlled by feedback. The range of stable discharge conditions is summarized in table 2. Experiments concentrated initially on ohmically heated discharges and have now been extended to include powerful ion cyclotron resonance and neutral beam injection heating. The ion cyclotron resonance heating operates at frequencies in the range 25 - 55 MHz corresponding to the gyro frequency resonances of H^+ and $^3He^{++}$ ions which are added as minority species to deuterium plasmas (typically in concentrations <10%). The position of the resonance layer and thus the power deposition profile can be varied either by changing the toroidal magnetic field or the frequency of the heating wave. Experiments started during 1985 using two antennas which could be connected in different configurations (monopole, dipole or octopole) to study how the coupling efficiencies varied with the distance between the plasma edge and the antennas. The maximum power coupled into the plasma was ~ 5MW for 2s. A third antenna was added early in 1986 and the coupled power is now being raised to towards 9MW. The central electron temperature rises to ~ 7.4keV.

Experiments with neutral beam injection started in 1986 with a single injection line capable of injecting up to about 6MW of 80keV H° or about 9MW of 80keV D° into the plasma. The maximum plasma temperature obtainable with neutral beam heating depends on the plasma density. At medium to high densities the ions have been heated to about 6.5keV and the electrons to 4.8keV using 5.5MW of neutral beam power. At lower densities the ion temperature can greatly exceed the electron temperature and can reach about 12.5keV.

Energy Confinement

Systematic studies have been made of the dependence of the global energy confinement time τ_E on various plasma parameters. In ohmic discharges the full range of plasma dimensions and elongations permitted by the JET vacuum vessel has been explored. This has included elongated full bore discharges (R = 2.96m, a = 1.2m, b/a $\lesssim$ 1.65) and circular discharges limited on the inner wall (R_0 = 2.5m, a = 0.8m). The latter discharges are a close simulation of discharges in TFTR and because of the strong gradient in B_T, have $B_T \simeq 4T$ on the plasma axis. As in smaller experiments the general trend of these data is that in ohmic discharges the confinement improves with increasing plasma density $\bar{n}_e$ and limiter safety factor q_a however, the JET data show a much weaker dependence on $\bar{n}_e$ and q_a than in smaller tokamaks (typically in JET $\tau_E \sim \bar{n}_e^{0.4} \times q_a^{0.3}$) and in particular the confinement time saturates for $n_e \gtrsim 3\ 10^{19}\ m^{-3}$. The regression fit to the full JET ohmic data set is

$$\tau_E = 0.03\ \bar{n}_e^{0.4}\ q_a^{0.3}\ B_T^{0.6}\ a^{1.3}\ R^{1.7}$$

Note that this linear fit to the full data set hides the saturation in n which is apparent when the data is examined closely. There is clearly a very strong dependence on the plasma dimensions ($\sim R^3$ at fixed R/a) and on toroidal field ($\sim B_T^{0.9}$ if the B_T dependence on q_a is included explicitly). It is also worth noting that there is no explicit dependence on the elongation b/a beyond that included implicitly in q_a. The largest value of τ_E in an ohmic discharge is $\tau_E \sim 0.8$ (I_p = 3MA, B_T = 3.4T).

With additional heating the confinement time τ_E degrades with increasing input power as seen in a number of other experiments. The degradation is independent of the type of heating, whether ion cyclotron, neutral beam or a combination of both. Figure 9 shows the plasma energy W_k plotted against

the total heating power P_T and can be represented by an offset linear scaling of the form $W = W(o) + \tau_{inc} P_t$. Where W(o) and the incremental confinement time τ_{inc} are functions of the plasma parameters. Extrapolating to higher heating powers, the global confinement time τ_E will saturate in the range 0.1 to 0.3s.

Recent experiments have produced magnetic separatrix configurations in JET (fig 10) which have improved confinement with neutral beam heating compared to limiter discharges. These discharges with improved confinement have many of the characteristics of the so-called H modes seen in other tokamaks.

Plasma Purity

The JET vacuum vessel is fabricated out of inconel (mainly nickel and chromium) and is usually operated at a temperature ~ 300°C. There are now eight large carbon limiters (0.8 x 0.4m) on the mid-plane at the outer major radius. The ion cyclotron antennas are in similar positions to the limiters but at slightly larger major radii and are surrounded by protective frames of carbon tiles. The inner wall is also covered with carbon tiles to a height of ± 1m above the mid plane. There are also carbon tiles at the top and bottom of the torus in the vicinity of the X points of the magnetic separatrix. The standard conditioning procedure following exposure of the torus to atomosphere is to bake the torus to about 350°C followed by several days of continuous glow discharge cleaning in hydrogen or deuterium.

The main impurities are carbon ($2\% \leq n_c/n_e \leq 4\%$) and oxygen ($1\% \leq n_o/n_e \leq 2\%$) which enter the discharge from the walls and limiters. The most important metallic impurity is nickel and the concentration is in the range 0.001 to 0.3% depending on the plasma conditions. The original sources of the nickel are the inconel walls and the nickel screens of the RF antennas. The nickel from the antennas is observed to enter the plasma directly when power is applied to an antenna but there is no influx from an antenna to which no power is applied. The nickel from the walls appears to enter the plasma by a two step process: (i) the carbon limiters become covered in metal during glow cleaning and following discharges which have ended with disruptions; (ii) during subsequent tokamak discharges this metal is eroded and enters the plasma. Thus we see that nickel concentrations in the plasma are reduced

progressively during a sequence of stable discharges with ohmic or neutral beam heating but are increased during ion cyclotron heated discharges or following discharges which have ended in disruptions. However, it is important to emphasize that under most conditions the concentration of metallic impurities in JET is small and does not significantly cool the central core of the discharge as shown in the radial profiles of the radiated power which were already illustrated in Figure 7.

The large area of carbon on the inside wall has a strong pumping effect and is used to control the plasma density by moving the discharge into contact with the inside wall. The detailed mechanism of this pumping effect is not yet fully understood.

Disruptions

Figure 11 summarizes the limits of stable operation in JET. The limit to low q operation is $q_\psi = 2.0 \geq 0.1$ where q_ψ is the field line q. The cylindrical q at the limiter ~ 1.6.

Disruptions at the density limit in discharges with $q_\psi \geq 3$ are preceded by signs of deterioration up to 1s before the final energy quench. The radiated power rises to equal the total power [31] and although the ohmic power also increases due to increased plasma resistance, it fails to keep place with the increasing radiation. The temperature profile contracts and there is increased mhd activity. In a typical case an oscillatory mode (predominantely m = 2, n = 1) grows for about 30ms and then the mode stops rotating and locks in a fixed toroidal phase. After the mode locks it continues to grow in amplitude and the ECE diagnostics show that the temperature profile flattens slightly at the minor radius corresponding to the calculated position of the q = 2 surface. This is consistent with the growth of a non-rotating magnetic island (the ECE diagnostic views close to the calculated position of the 'O' point). There are indications of similar evidence from the soft x-ray diode diagnostics but the analysis is presently at a preliminary stage and there could be other interpretations. The spatial resolution of the ECE diagnostic (at present 40mm in the radial direction) is not quite sufficient to determine whether the 'O' point of the magnetic island is colder than the surrounding plasma as predicted by one model of disruptions. The new superheterodyne ECE diagnostic will have better spatial resolution and will be used for these

studies. The soft x-ray diode arrays give a very detailed picture of the displacement of the hot central core in the final few ms before the energy quench.

Sawteeth

Sawtooth oscillations occur in almost all discharges and have been studied extensively with a range of diagnostics [31]. In ohmically heated plasmas the modulation of the central electron temperature is up to 20% and the period is between 30 and 250 ms. In discharges with ion cyclotron heating (Figure 12) or co-injected neutral beams the modulation is increased up to 50% and the period extended up to 600ms, whereas with counter injected beams both the modulation and the period are reduced. With combined ion cyclotron and neutral beam heating we have sometimes seen sawteeth of very long duration lasting for more than 1s. These have been called "monster" sawteeth. The monster sawteeth were first seen in relatively low current discharges (I_p ~ 2MA) but similar long duration monster sawteeth have now been seen in discharges with an internal separatrix (I_p = 2MA) and at high currents I_p = 5MA (Figure 13). These are not simply sawteeth with particularly long periods but they are characterised by low levels of coherent mhd activity suggesting that the internal m = 1 mode has stabilized. However, after a monster sawtooth collapses the plasma remains in an unstable state which seems to prevent the growth of a second monster sawtooth in the same discharge although they may be several more normal sawteeth.

The collapse mechanism appears to be the same in all JET discharges although there is a range of different precursor activity. The collapse occurs on a much shorter time scale (typically about 100μs) than would be consistent with resistive reconnection models. Detailed studies with the x-ray and ECE diagnostics show that the collapse has an m = n = 1 structure and involves the displacement in minor radius of the hot central core of plasma. The displaced core spreads poloidally around the magnetic axis into a crescent shaped region [30] and at the same time there is a rapid outflow of plasma energy. The time scale of the collapse together with the detailed displacement and spreading of the hot core are in agreement with the predictions of a model where the sawtooth collapse is an ideal mhd instability.

4. Future Plans

The programme planned for JET includes a substantial increase in the additional heating power. During the next three years the ion cyclotron heating will be increased to 15MW for 20s. A second neutral beam line will be installed in 1987 to bring the total neutral beam power to about 10MW of 80keV H°, 160keV D° or about 18MW 80keV D°. This additional heating power will be tested in two discharge configurations: a) a magnetic separatrix at $I_p \lesssim$ 4MA, b) limiters at $I_p \lesssim$ 7MA (such a low q discharge has already been simulated at 3.5MA and B_T = 1.7T). The main aim of JET experiments during the next few years will be to reach maximum performance with full additional heating power in deuterium plasmas before proceeding to the final phase requiring the introduction of tritium. A number of other machine enhancements which might influence the confinement are also being considered. These include control of the current profile using lower hybrid resonance heating, beryllium limiters and gettering, feedback control of disruptions and repetitive hydrogen pellet injection.

Very few major diagnostics are planned for JET beyond those which are already in construction. However there are a few minor additions (including a laser blow-off system to inject trace impurities) and several modifications and upgrades to existing systems. Them include upgrading the Far-Infra-Red interferometer permit Faraday Rotation measurements (KG4), and various ideas for α particle diagnostics.

5. Conclusion

A considerable effort has been invested into providing the JET experiment with a comprehensive set of diagnostics. Particular emphasis has been placed on making measurements of the different plasma parameters simultaneously within a single discharge, in order to avoid problems of irreproducibility. Considerable care has been taken during the design and construction of these diagnostic systems to ensure that they are consistent with the high standards of engineering of other systems of the JET machine. Many of the systems described in this paper were operated in a preliminary version for the first operation of JET in 1983, and since then they have been refined and brought into full operation, allowing the scientific personnel to concentrate on interpretation of data. A few systems including the neutron diagnostics

specifically intended for the later phases of JET's programme are still in construction and will be installed within the next few years.

Acknowledgements

The successful implementation of the JET diagnostic systems is due to the efforts of many colleagues in the JET Team, and in the other European Fusion Laboratories. I am grateful for their contributions and hard work.

References

[1] The JET Team., IAEA Conf. on Plasma Physics and Controlled Nuclear Fusion Research, Kyoto, Japan, 1986. Paper CN-47/A-I-2.

[2] J Jacquinot et al, IAEA Conf. on Plsma Physics and Controlled Nuclear Fusion Research, Kyoto, Japan, 1986. Paper No. 28, 1 (1986).

[3] P P Lallia et al, IAEA Conf. on Plasma Physics and Controlled Nuclear Fusion Research, Kyoto, Japan, 1986. Paper No. 28, 1211 (1986).

[4] The JET Team, First Results of Neutral Beam Heating on JET., Plasma Physics and Controlled Fusion., Vol 28 No. 9A P.1429 (1986).

[5] P E Stott, Course on Diagnostics for Fusion Reactor Conditions, Varenna, Italy, 1982. Vol. II P517.

[6] J P Christiansen, Integrated Analysis of Data from JET, JET Report, JET-R(86)04.

[7] P E Stott, Course on Diagnostics for Fusion Reactor Conditions, Varenna, Italy, 1982. Vol.II P403.

[8] D Veron, Course on Diagnostics for Fusion Reactor Conditions, Varenna, Italy 1982. Vol.I P199.

[9] G Magyar & J O'Rourke, Operating the JET Multichannel FIR Interferometer, this Conference.

[10] A E Costley, Diagnosis of Fusion Plasmas Using Reflectometry, this Conference.

[11] A Hubbard et al, Electron Density Measurements on JET using a Microwave Reflectometer, this Conference.

[12] R Prentice et al, The JET Multichannel Reflectometer, this Conference.

[13] D Pasini et al, The X-ray Pulse Height Analysis System at JET, this Conference.

[14] A E Costley, Recent Developments and Applications of Electron Cyclotron Emission, this Conference.

[15] N Salmon et al, An Electron Cyclotron Emission Diagnostic for the Edge Region of the JET Plasma, this Conference.

[16] P Nielsen et al, The Single Point Thomson Scattering System for JET, (to be published).

[17] R Prentice et al, First Results from Thomson Scattering on JET. Proc. 5th Topical Conf. on High Temperature Plasma Diagnostics, Tahoe City, USA, Sept. 1984. Rev. Sci. Insts. Vol.56 No.5 ptII P1070 (1985) Abstract.

[18] C Gowers et al, The JET LIDAR Thomson Scattering System, this Conference.

[19] G Bracco, S Corti, V Zanza et al, First Results from JET Neutral Particle Analyser (NPA) (1984), JET-IR(84)04.

[20] O N Jarvis et al, Neutron Spectrometry at JET., 6th Topical Conf. on High Temperature Plasma Diagnostics. Rev. Sci. Instr. 57 (1986) 1717.

[21] S Bombarda, R Giannella, E Kallne, G Tallents, S Bly-daubah, P Faucher, M Cornille, J Dubah and A H Gabriel, Observations and Comparisons with Theory of Helium and Hydrogen - Like Spectra of Nickel from the JET Tokamaks, (to be published).

[22] M Von Hellermann, Charge Exchange Recombination Spectroscopy on JET., this Conference.

[23] K Behringer, B Denne & G Magyar, Space Resolved Measurment of Impurity Radiation on the JET Tokamak, this Conference

[24] R Behrisch et al, Contamination of the JET Limiters with Metals during the Different Operational Phases., 7th Int. Conf. of Plasma Surface Interactions in Fusion Devices, Princeton, USA (1986). (JET-P(86)35).

J P Coad et al, Depth Profiling Experiments on JET Wall Samples., 7th Int. Conf. of Plasma Surface Interactions in Fusion Devices, Princeton, USA (1986). (JET-P(86)35).

[25] T Tagle, Diagnosis of the JET Scrape-off Layer using heat flux/Langmuir Probes, this Conference

[26] D Summers, Thermography of Carbon Limiters, this Conference

[27] C Lowry, The Limiter as a passive Diagnostic, this Conference

[28] D B Syme, Neutron Diagnostics for JET, this Conference

[29] G. Sadler et al, Fusion Product Measurements on JET, 13th Euro. Conf. on Controlled Fusion & Plasma Heating, Schliersee, April 1986, Vol 10C (1986) 105.

[30] R Granetz, X-ray Tomography and the Physics Results from JET (Abstract only), this Conference

[31] D Campbell et al, IAEA Conf. on Plasma Physics and Controlled Nuclear Fusion Research, Kyoto, Japan, 1986. IAEA CN 47/A VII-5

[32] The JET Team, IAEA Conf. on Plasma Physics and Controlled Nuclear Fusion Research, Kyoto, Japan, 1986. IAEA CN 47/A-1-2.

Table 1

STATUS OF THE JET DIAGNOSTICS SYSTEMS, OCTOBER 1986

System	Diagnostic	Purpose	Association	Status (OCT. '86)	Compatibility with tritium	Level of automation
KB1	Bolometer Scan	Time and space resolved total radiated power	IPP Garching	Operational	Yes	Semi-automatic
KC1	Magnetic Diagnostics	Plasma current, loop volts, plasma position, shape of flux surfaces	JET	Operational	Yes	Fully automatic
KE1	Single Point Thomson Scattering	T_e and n_e at one point several times	Risø	Operational	Yes	Fully automatic
KE3	Lidar Thomson Scattering	T_e and n_e profiles	JET and Stuttgart University	Being installed Operational mid '87	Yes	Will be fully automatic
KG1	Multichannel Far Infrared Interferometer	$\int n_e ds$ on 7 vertical chords and 3 horizontal chords	CEA Fontenay-aux-Roses	Operational	Yes	Semi-automatic
KG2	Single Channel Microwave Interferometer	$\int n_e ds$ on 1 vertical chord	JET and FOM Rijnhuizen	Operational	Yes	Fully automatic
KG3	Microwave Reflectometer	n_e profiles and fluctuations	JET	(1) Prototype system operational (2) Multichannel system being constructed. Operational mid '87	Yes	(1) Not automatic (2) Will be fully automatic
KG4	Polarimeter	$\int n_e B_\phi ds$ on 6 vertical chords	CEA Fontenay-aux Roses	Operational early '87	Yes	Semi-automatic
KH1	Hard X-ray Monitors	Runaway electrons and disruptions	JET	Operational	Yes	Fully automatic
KH2	X-ray Pulse Height Spectrometer	Plasma purity monitor and T_e on axis	JET	Operational	Yes, after modification	Semi-automatic
KJ1	Soft X-ray Diode Arrays	MHD instabilities and location of rational surfaces	IPP Garching	Operational	No	Semi-automatic
KK1	Electron Cyclotron Emission Spatial Scan	T_e (r,t) with scan time of a few milliseconds	NPL, UKAEA Culham and JET	Operational	Yes	Fully automatic
KK2	Electron Cyclotron Emission Fast System	T_e (r,t) on microsecond time scale	FOM, Rijnhuizen	Operational	Yes	Fully automatic
KL1	Limiter surface temperature	Monitor of hot spots on limiter, walls and RF antennae	JET and KFA Jülich	Operational	No	Fully automatic
KL2	Limiter surface temperature	Temperature of belt limiters	JET	Under construction	No	Will be fully automatic
KM1	2.4MeV Neutron Spectrometer	Neutron spectra in D-D discharges, ion temperatures and energy distributions	UKAEA Harwell	Not yet fully operational	Yes	Will be fully automatic
KM3	2.4MeV Time-of-Flight Neutron Spectrometer		NEBESD, Studsvik	Not yet fully operational	Yes	Will be fully automatic
KM4	2.4MeV Spherical Ionisation Chamber		KFA Jülich	Not yet installed	Yes	Will be fully automatic
KM2	14MeV Neutron Spectrometer	Neutron spectra in D-T discharges, ion temperatures and energy distributions	UKAEA Harwell	Design completed	Yes	Not yet installed
KM5	14MeV Time-of-Flight Neutron Spectrometer		NEBESD, Gothenberg	Decision on construction under review	Yes	Not yet installed
KN1	Time Resolved Neutron Yield Monitor	Time resolved neutron flux	UKAEA Harwell	Operational	Yes	Fully automatic
KN2	Neutron Activation	Absolute fluxes of neutrons	UKAEA Harwell	Commissioning	Yes	Not yet implemented
KN3	Neutron Yield Profile Measuring System	Space and time resolved profile of neutron flux	UKAEA Harwell	Commissioning	Yes	Not yet implemented
KN4	Delayed Neutron Activation	Absolute fluxes of neutrons	Mol	Awaiting delivery	Yes	Not yet installed
KP1	Fusion Product Detectors	Charged particles produced by fusion reactions	JET	Prototype operational	Prototype - No	Prototype not automatic
KR1	Neutral Particle Analyser Array	Profiles of ion temperature	ENEA Frascati	Operational	Yes, after modification	Semi-automatic
KS1	Active Phase Spectroscopy	Impurity behaviour in active conditions	IPP Garching	Operational early '87	Yes	Not yet implemented
KS2	Spatial Scan X-ray Crystal Spectroscopy	Space and time resolved impurity density profiles	IPP Garching	Operational end '86	No	Not yet implemented
KS3	H-alpha and Visible Light Monitors	Ionisation rate, Z_{eff}, Impurity fluxes	JET	Operational	Yes	Semi-automatic
KS4	Charge Exchange Recombination Spectroscopy (using heating beam)	Fully ionized light impurity concentration, $T_i(r)$, rotation velocities	JET	Operational	Yes	No
KT1	VUV Spectroscopy Spatial Scan	Time and space resolved impurity densities	CEA Fontenay-aux-Roses	Operational	No	Semi-automatic
KT2	VUV Broadband Spectroscopy	Impurity survey	UKAEA Culham	Operational	No	Fully automatic
KT3	Visible Spectroscopy	Impurity fluxes from wall and limiters	JET	Operational	No	Semi-automatic
KT4	Grazing Incidence Spectoscopy	Impurity survey	UKAEA Culham	Operational	No	Semi-automatic
KX1	High Resolution X-ray Crystal Spectroscopy	Ion temperature by line broadening	ENEA Frascati	Operational	Yes	Fully automatic
KY1	Surface Analysis Station	Plasma wall and limiter interactions including release of hydrogen isotope recycling	IPP Garching	Operational	Yes	Automated, but not usually operated unattended
KY2	Surface Probe Fast Transfer System		UKAEA Culham	Operational	Yes	
KY3	Plasma Boundary Probes	Vertical probe drives for electrical and surface collecting probes	JET, UKAEA Culham and IPP Garching	Operational	No	
KZ1	Pellet Injector Diagnostic	Particle transport, fuelling	IPP Garching	Operational	Yes	Not automatic

Table II
Range of the Main JET Plasma Parameters

Parameter	Value
Toroidal field (plasma centre) B_t	1.7-3.4 T
Plasma current, I_p	1-5 MA
Flux safety factor at edge, q_ψ	2.2-16
Volume averaged density, $\bar{n}_e$	$0.5\text{-}5\times10^{19}\,\mathrm{m}^{-3}$
Central electron temperature, $\hat{T}_e$	2-7.5 keV
Central ion temperature, $\hat{T}_i$	1.5-12 keV
Energy confinement time, τ_E	0.2-0.9 s

Location of J.E.T. Diagnostic Systems

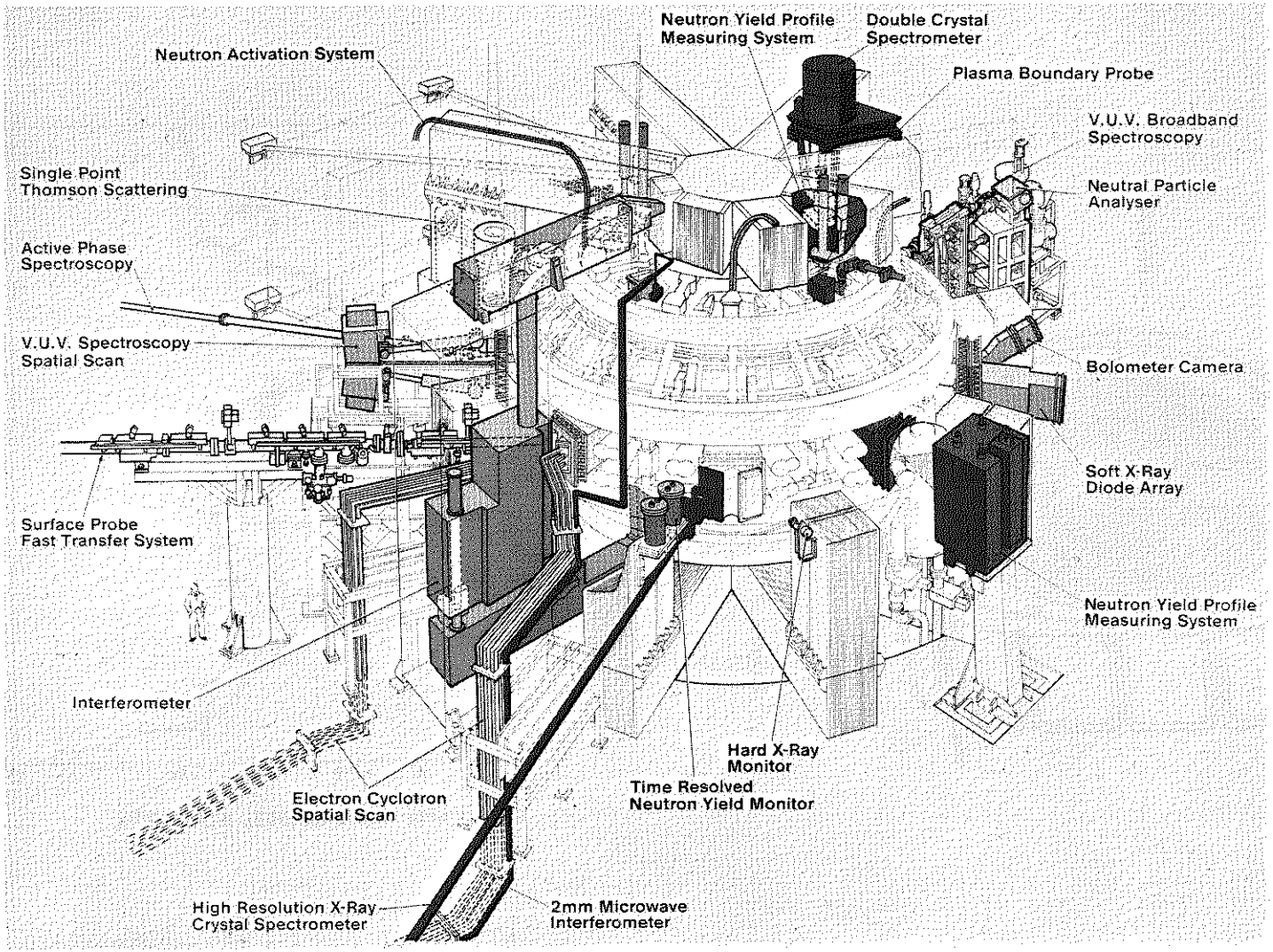

Figure 1 Schematic showing the location of some of the JET Diagnostic Systems.

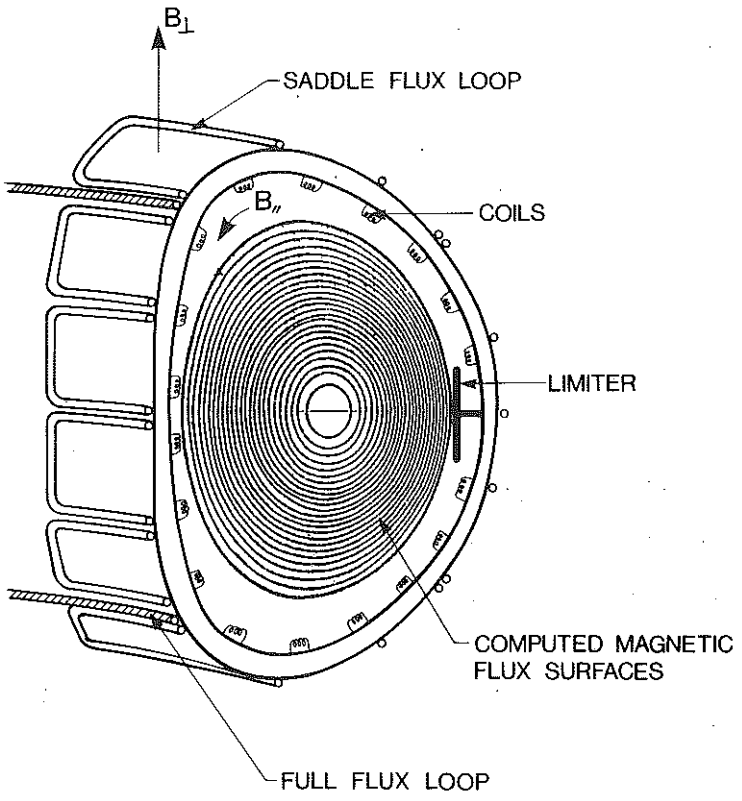

Figure 2 Magnetic diagnostics.

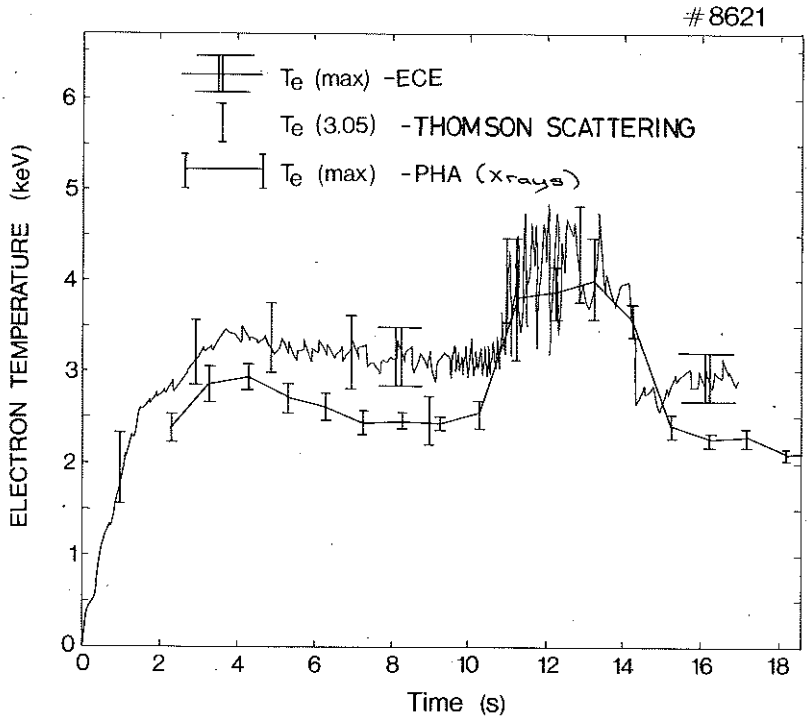

Figure 3 Comparison of Electron Temperature Measurements with different diagnostics.

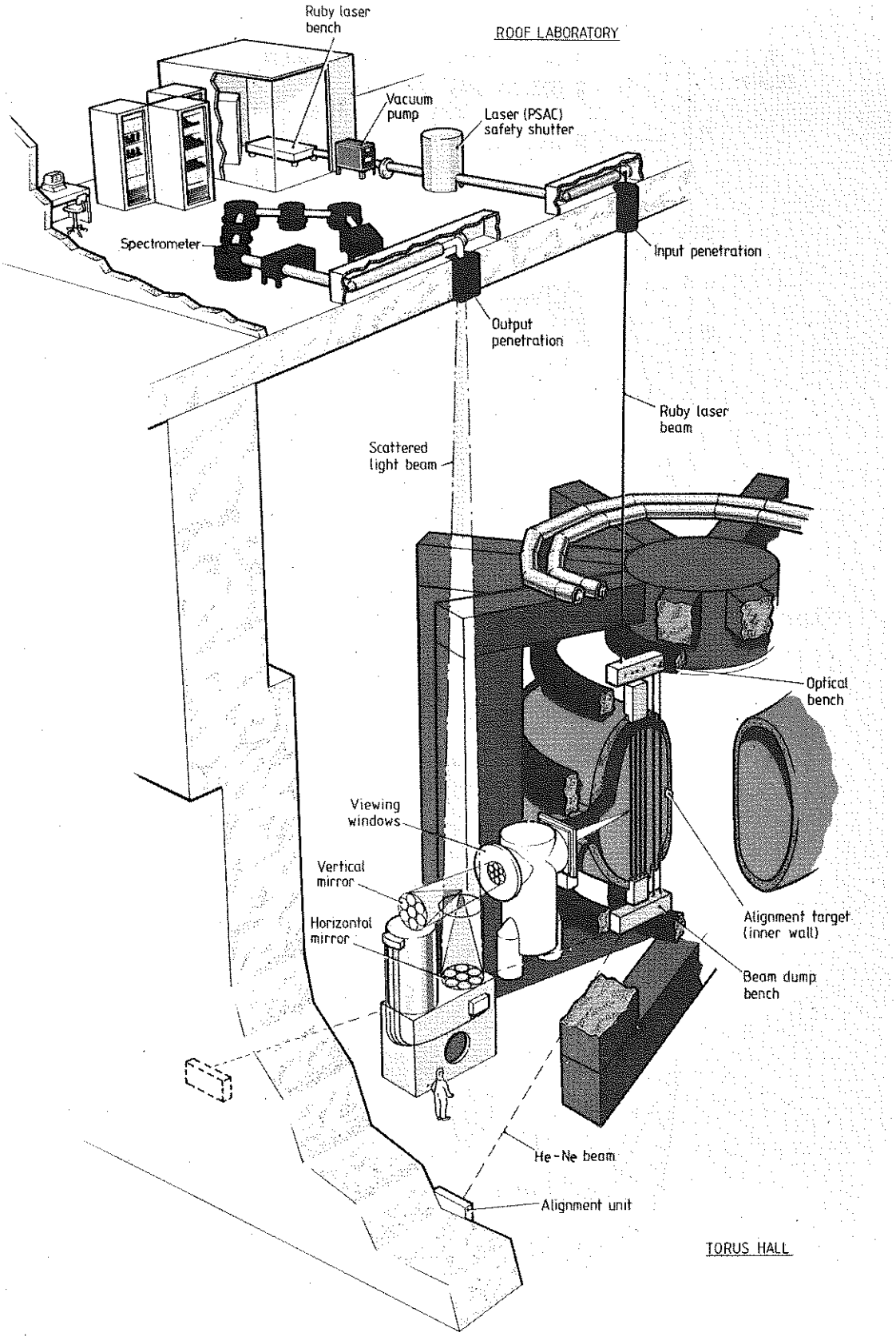

SINGLE POINT THOMSON SCATTERING SYSTEM KE1

Figure 4 Schematic of the Single Point Thomson Scattering Diagnostic.

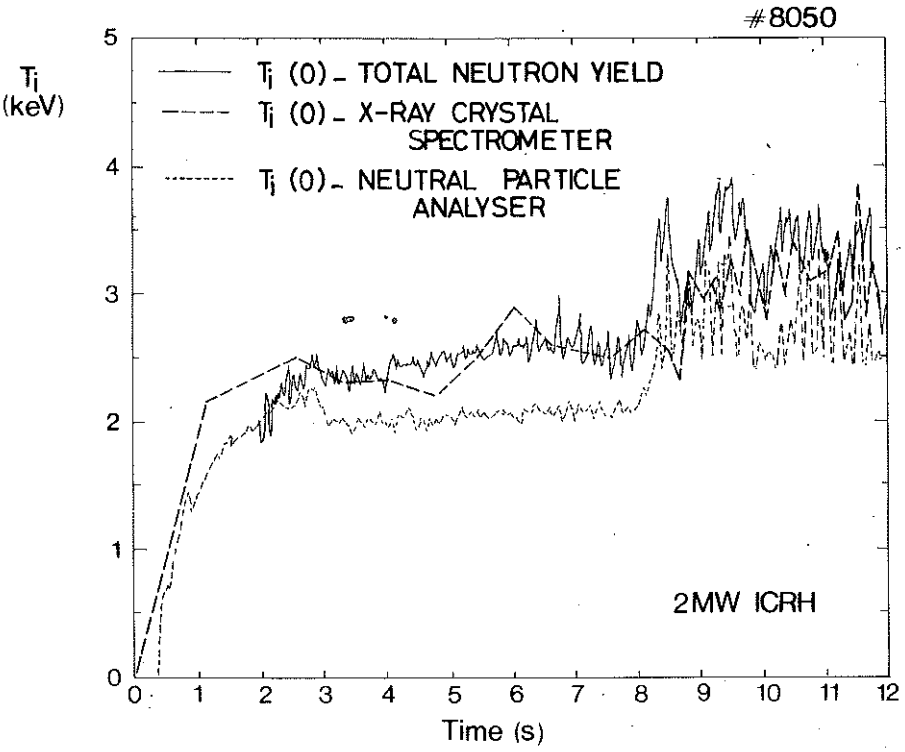

Figure 5 Comparison of Ion Temperature Measurements with different diagnostics.

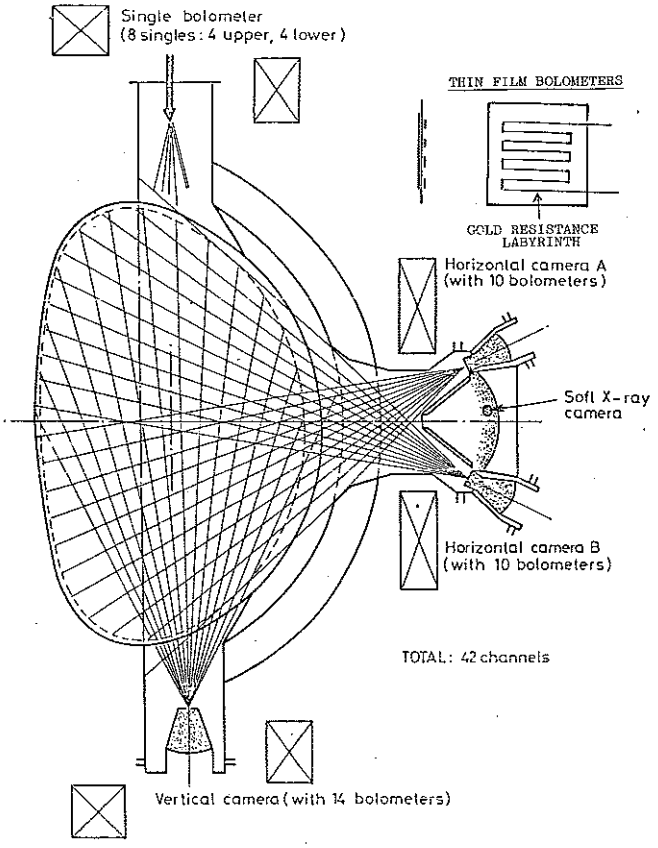

Figure 6 Lines of sight of the bolometer arrays.

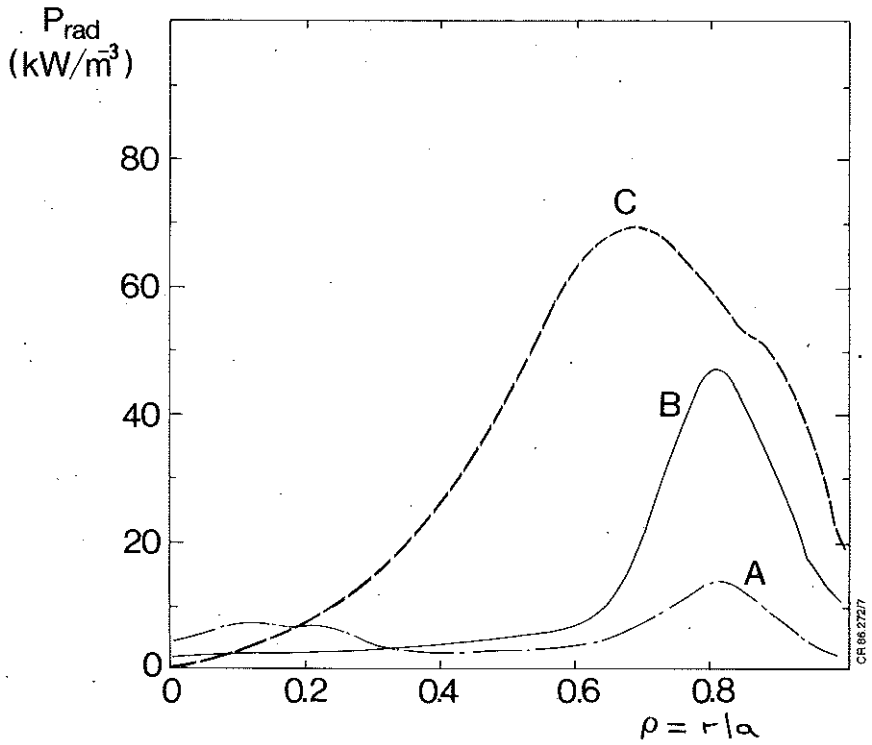

Figure 7 Profiles of radiated power density measured with the bolometer arrays.

A = a typical ohmic discharge

B = an NBI discharge located on the inner wall

C = a combined heating discharge on the limiter

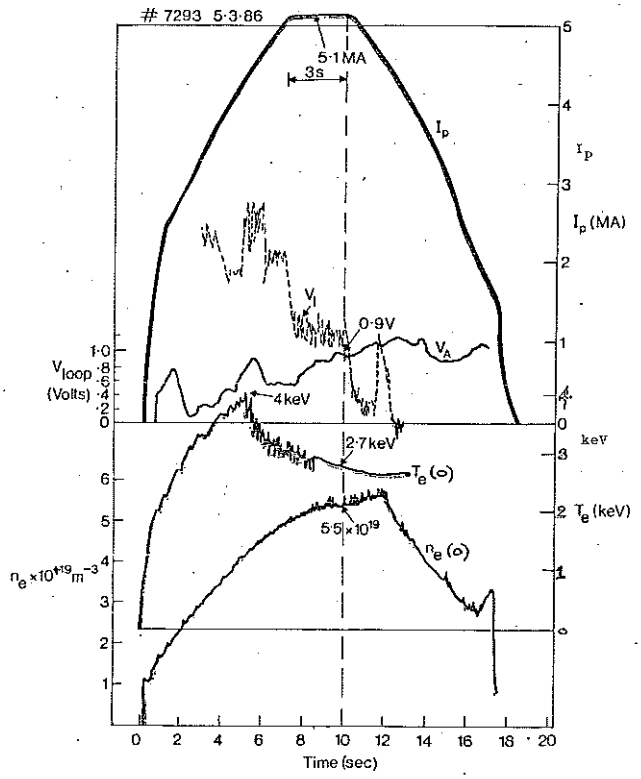

Figure 8 Waveforms of current, and central electron temperature and density in a high current ohmic discharge (B_T=3.4T, q_ψ=3.25, q_{cyl}=2.25, b/a=1.4).

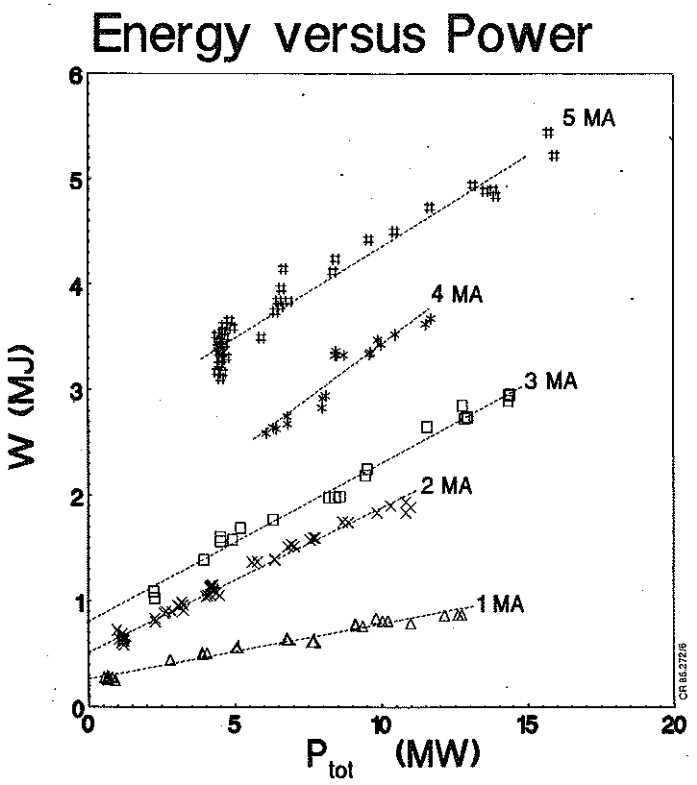

Figure 9 Total plasma energy versus total input power for discharges with different plasma currents (D_p 1 < I_p < 5MA) and additional heating.

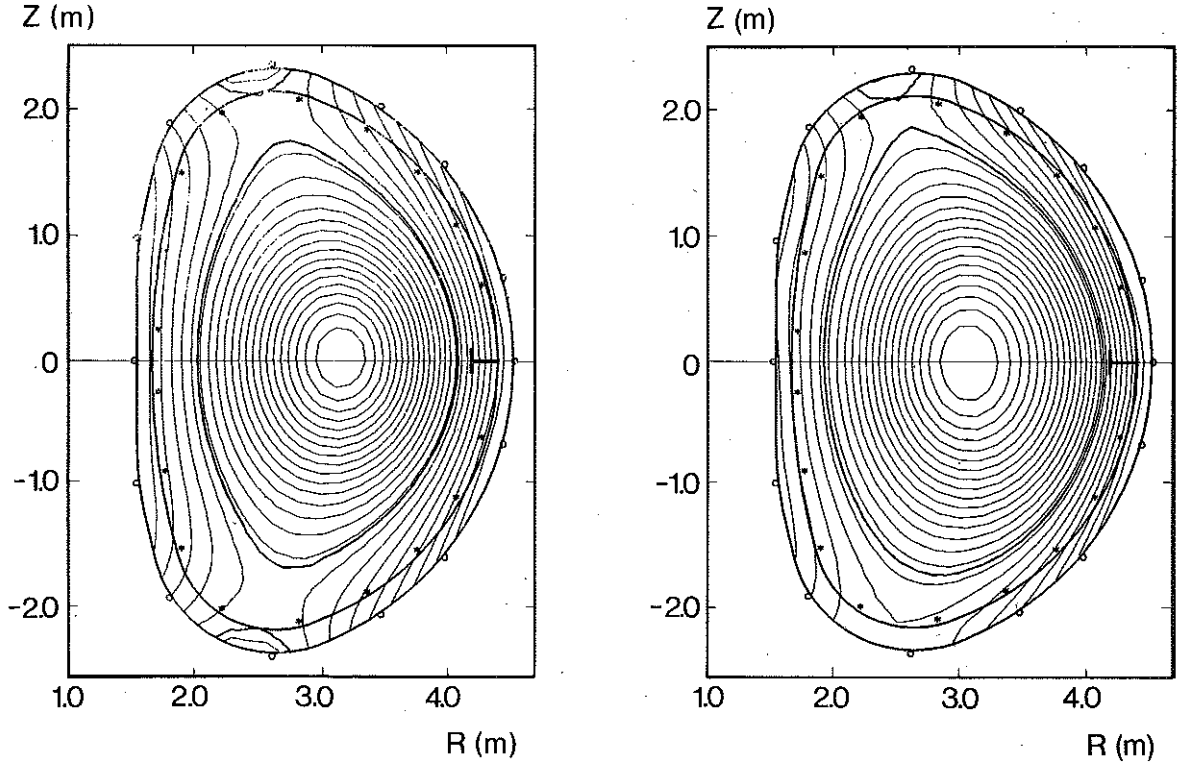

Figure 10 Magnetic flux surfaces for discharges with internal separatrices showing double and single null configurations.

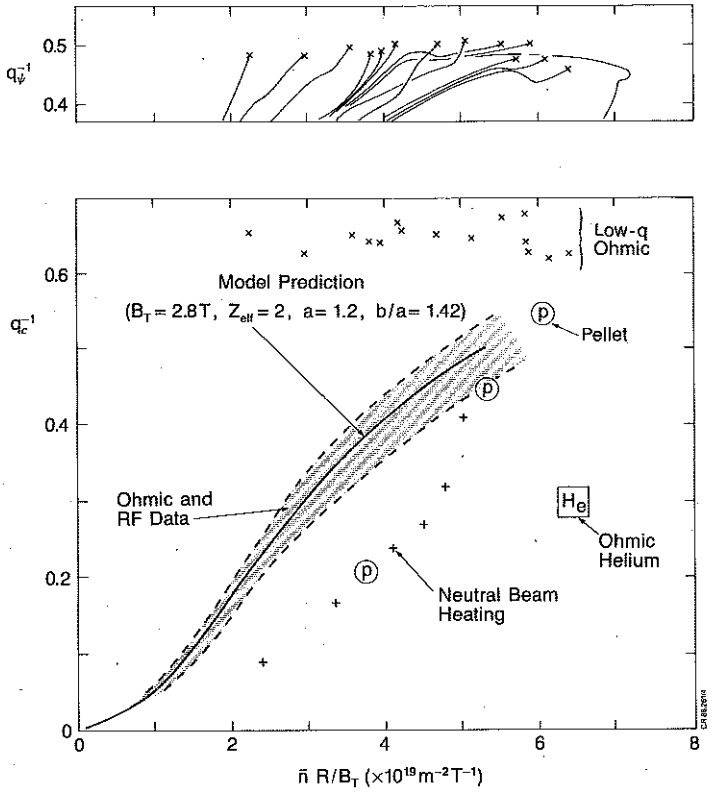

Figure 11 Hugill diagrams showing the limits of stable operation.

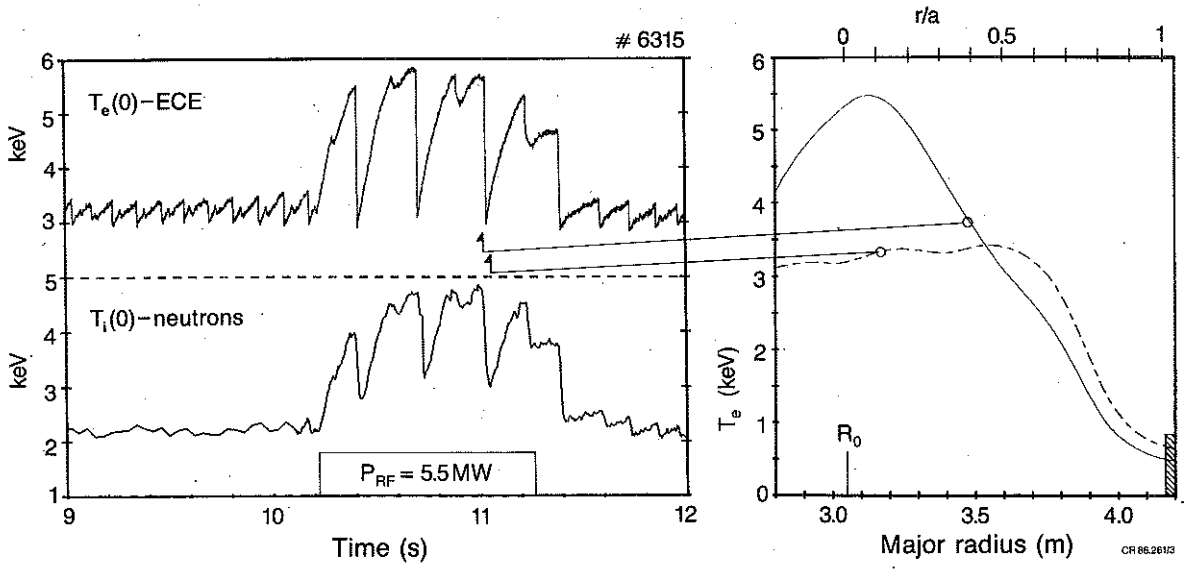

Figure 12 Sawteeth in a discharge with ion cyclotron heating.

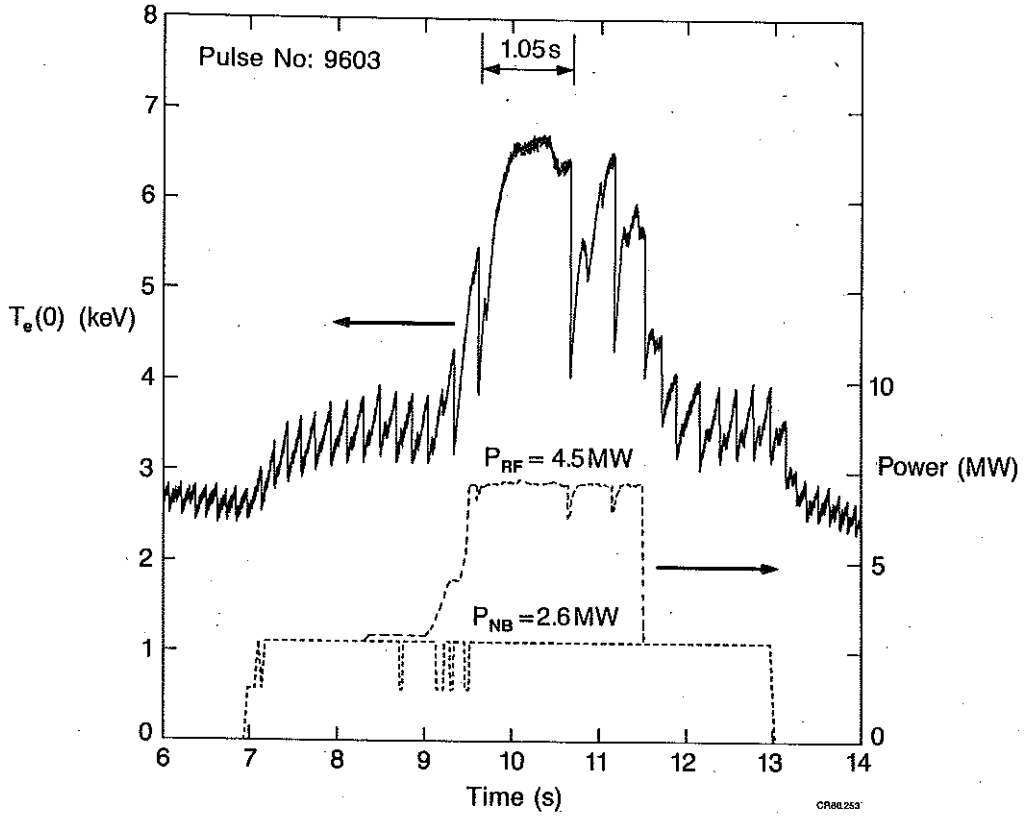

Figure 13 Monster sawtooth in a discharge with combined neutral beam and ion cyclotron heating.